

RESEARCH ARTICLE

Molecular Interactions of Zyesami with the SARS-CoV-2 nsp10/nsp16 Protein Complex

Sultan F. Alnomasy^{1*}, Bader S. Alotaibi¹, Ziyad M. Aldosari¹, Ahmed H. Mujamammi², Ahmad Alzamami¹, Pragya Anand³, Yusuf Akhter³, Farhan R Khan¹ and Mohammad R. Hasan¹

¹Department of Medical Laboratory Sciences, College of Applied Medical Sciences in Al-Quwayiyah, Shaqra University, Saudi Arabia; ²Department of Pathology, Clinical Biochemistry Unit, College of Medicine, King Saud University, Riyadh, Saudi Arabia; ³Department of Biotechnology, Babasaheb Bhimrao Ambedkar University, Vidya Vihar, Raebareli Road, Lucknow, India

Abstract: Background: SARS-CoV-2 emerged in late 2019 and caused COVID-19. Patients treated with Zyesami were found to have a 3-fold decrease in respiratory failure and improved clinical outcomes. It was reported that Zyesami inhibits RNA replication of SARS-CoV-2, including several non-structural proteins essential in viral RNA replication. SARS-CoV-2 is a distinctive virus that requires nsp10 and nsp16 for its methyltransferases activity which is crucial for RNA stability and protein synthesis.

Objective: We aimed the *in silico* determination of inhibitory consequences of Zyesami on the SARS-CoV-2 nsp10/nsp16 complex. Targeting SARS-CoV-2 nsp10/ nsp16 protein complex may be used to develop a drug against COVID-19.

Methods: I-TASSER was used for secondary structure prediction of Zyesami. CABS-dock was used to model Zyesami with SARS-CoV-2 nsp16 interaction. The docked complex was visualized using PyMol. The quality of the docking model was checked by using ProQdock.

Results: The 3D structure of SARS-CoV 2, nsp10/nsp16 showed that essential interactions exist between nsp10 and nsp16. Significant contact areas of Zyesami exist across amino acid residues of nsp10; Asn⁴⁰-Thr⁴⁷, Val⁵⁷-Pro⁵⁹, Gly⁶⁹-Ser⁷², Cys⁷⁷-Pro⁸⁴, Lys⁹³-Tyr⁹⁶. In addition, polar contacts between nsp16 and Zyesami are Asn²⁹⁹-Ser⁴⁴⁰, Val²⁹⁷-Asn⁴⁴³, Gly¹⁴⁹-Tyr⁴³⁷, Gln¹⁵⁹-Lys⁴³⁰, Asn¹⁷⁸-Arg⁴²⁹, Ser¹⁴⁶-Arg⁴²⁹, Ser¹⁴⁶-Arg⁴²⁹, Lys¹⁴⁷-Arg⁴²⁹, Asr²²¹-Thr⁴²², Lys¹⁸³-Asp⁴²³, Lys¹⁸³-Asp⁴²³, and Gln²¹⁹-Asp⁴²³ the residues are shown of nsp16 and Zyesami respectively.

Conclusion: The structural bioinformatics analyses have indicated the potential binding specificity of Zyesami and nsp16. Data predict how the initial binding of Zyesami with nsp10 and nsp16 may occur. Moreover, this binding could significantly inhibit the 2'-O-MTase activity of the SARS-CoV nsp10/16 complex.

Keywords: COVID-19, SARS-CoV-2, Microbiology, Zyesami, Coronavirus, nsp16, nsp10.

1. INTRODUCTION

Severe acute respiratory syndrome coronavirus 2 (SARS-CoV-2) causes a disease which is known as COVID-19. In the fight against this virus, researchers have come up with three options for developing new drugs: [1]. The first option is to examine current broad-spectrum anti-viral drugs [2]. The second option is to use present molecular databases to find molecules that affect coronavirus [3]. The third option starts from scratch to develop new drugs based on the

genomic information of different coronaviruses [4]. Zyesami is a synthetic, vasoactive intestinal polypeptide (VIP). The trade name is Aviptadil, RLF-100. Zyesami and pituitary adenylate cyclase-activating polypeptide (PACAP) are synthetic forms of VIP. It is known that VIP is produced by neuroendocrine cells, T and B cells, and is found in high concentrations in the lungs also. VIPs are reported to inhibit the replication of SARS-CoV-2 in lung epithelial cells and monocytes [5]. These VIPs are involved in the control of human intestine motility as well as immune system regulation [6]. The VIP peptide comprises 28-amino acid residues, which were discovered by Said and Mutt in 1970 [7]. On the other hand, PACAP is a 38-amino acid long peptide isolated

*Address correspondence to this author at the Department of Medical Laboratory Sciences, College of Applied Medical Sciences in Al-Quwayiyah, Shaqra University, Saudi Arabia; E-mail: s.alnomasy@su.edu.sa

from the ovine hypothalamus in 1989 [8]. VIP interacts with VIP receptor type-1 (VPAC1), present mainly in the lungs and T-lymphocytes, which are GPCR-type receptors. The mechanism of action of these peptides is to increase the production of cyclic AMP in cells [9]. SARS-CoV-2, like other coronaviruses, uses S1 and S2 spike proteins on the envelope to bind to their cellular receptors, leading to a cascade of fusion between viral membranes and cells for cell entry. The SARS-CoV spike protein and its interaction with the cell receptor ACE2 is a critical initial step for SARS-CoV to enter target cells [26]. Furthermore, *in vitro* studies showed that the binding of SARS-CoV-2 RBD to ACE2 with high affinity suggests that the RBD is a functional component within the S1 subunit responsible for the binding of SARS-CoV-2 by ACE2 [26-28, 32], [10, 11]. Further studies reported that not only ACE2 but also neuropilin (NRP1) act as SARS-CoV-2 host cell receptors implicated in the entry of SARS-CoV-2 into human cells [12, 29, 30] and using host machinery, the virus starts its RNA replication within the host. The virus's specific molecular interaction with the host cell signifies a promising therapeutic target for identifying SARS-CoV-2 antiviral drugs. GNF-5, RS504393, GR 127935, hydrochloride hydrate, TNP, and eptifibatide acetate are drugs against SARS-CoV-2. Many compounds have been identified as drugs whose target is the viral binding site of the ACE2 receptor. [34-36]. For example, eptifibatide acetate interacts with ACE2 through 3H-bonds with residues His34, Glu75, and Gln76, and hydrophobic bonds with Lys31, Glu35, Asp38, Leu39, Lys68, and Phe72 that could block interactions of the SARS-CoV-2-ACE2 receptor [31]. A protein-protein docking model based on the S1-subunit of SARS-CoV-2 used to identify molecular interactions with the ACE2 receptor found hotspot 31 and hotspot 353 as central residues of S-RBD residues. Docking calculations suggest that the S-RBD residues of SARS-CoV-2 interacting with the ligands are Leu455, Phe486, Asn487, Gln493, and Ser494. The residues Leu455, Phe486, and Gln493 of S-RBD interact with hotspot 31. However, Asn487 and Ser494 are known to interact with hotspot 353 [33]. KT203- a drug molecule that interacts with S-RBD residues through one hydrogen bond with O3-O(Phe490)- Hydrophobic interactions Tyr449, Asn450, Tyr451, Leu452, Leu455, Lys458, Phe486, Tyr489, Pro491, Leu492, Gln493, Ser494 [31]. KT203 and BMS195614 displayed a maximum number of hydrophobic interactions with residues responsible for recognizing hotspot 31 and hotspot 353 [31]. Further, KT203 binds with Leu455, Phe486, Tyr489, Gln493, and Ser494 through hydrophobic interactions, all known to be a part of the virus binding motif of the ACE2 receptor. The SARS-CoV-2 RNA replication machinery includes several non-structural proteins (nsp) that play fundamental roles in the synthesis and replication of the virus RNA. Nsp7/nsp16 are involved in the capping of viral RNA [13]. In conjunction with nsp10, a critical cofactor for SARS-CoV-2, nsp16 functions as a 2'-O-methyltransferase (MTase) [14]. This nsp10/nsp16 complex is necessary to ensure viral RNA integrity against host immune response [15, 16], indicating it as a potential therapeutic target. In this work, an *in silico* analysis of Zyesami's interaction with SARS-CoV-2 nsp16 was performed to learn more about nsp16, a new anti-SARS-CoV-2 target. Hence, this computational approach would assist in providing more target information against SARS-CoV-2 therapeutic intervention.

2. MATERIALS AND METHODS

2.1. Secondary Structure Prediction and Potential Binding Sites of Zyesami

The amino acid sequence of Zyesami (HSDALFXDX YXRLRKQMAMKKYLNSVLN) was used to predict the secondary structure and possible binding sites within Zyesami using Iterative Threading ASSEMBLY Refinement (I-TASSER) from (<http://zhanglab.ccmb.med.umich.edu/I-TASSER/>). I-TASSER generated the modelled peptide structure of 28 amino acid residues, where the first identified structure of this peptide by Local Meta-Threading-Server (LOMETS) was used. Following this, the 3D model of Zyesami was prompted for protein-protein docking using BioLiP (<https://zhanggroup.org/BioLiP/>).

2.2. Modelling of Zyesami with SARS-CoV-2 nsp16 Interaction

The tertiary structure of the target protein (PDBID_6W4H) for the nsp16-nsp10 complex from SARS-CoV-2 was obtained from Protein Data Bank (PDB) (www.rcsb.org) database, and the peptide sequence for Zyesami was retrieved from PDB database. The amino acid sequence of Zyesami and PDB file was submitted to CABS-dock [17] for docking Zyesami against SARS-CoV-2 nsp16. CABS-dock does not require prior binding site information and predicts 75.4% residues [17]. As input, it requires a PDB file and FASTA sequence. Protein-peptide docking was done based on interaction similarity. The required input is the target protein in PDB format (6W4H), and the peptide sequence was saved in FASTA format for input. CABS-dock has a size range limited to 900 and 30 amino acids for protein structure and peptide. The docked complex was visualized using PyMol 2.4.1 for interaction analysis. The quality of the docking model was finally checked by using ProQdock [18].

3. RESULTS

3.1. Docking Model of Zyesami's Interaction with the SARS-CoV-2 nsp10/nsp16 Complex

The three-dimensional structure of nsp16 (6W4H) was used as the target protein in the molecular interaction studies. The crystal structure, 6W4H, determined by X-ray diffraction, shows that nsp16 is complexed with non-structural protein nsp10. In addition, nsp10 plays an important role as a cofactor for other non-structural proteins in SARS-CoV-2, which Laurini also reports. SARS-CoV-2, nsp10/nsp16 (6W4H) is a heterodimer complex that is necessary for capping viral mRNA transcripts for effective translation of coronavirus RNA [19, 24, 25]. The nsp10/nsp16 system is also essential for preventing immune recognition [15, 16]. Therefore, this work was carried out to identify binding sites of Zyesami against SARS-CoV-2/COVID-19 nsp16. For this purpose, CABS-dock was used to dock Zyesami within nsp16 of SARS-CoV-2/COVID-19 (accession number 6W4H: A). The amino acid sequence of Zyesami was submitted to CABS-dock. ProQdock was used to check the quality of the docking model [18]. CABS-dock generated several docking models, and then ProQdock was used to rank these models according to their quality score, and only

the top-scored model was used in this work (Fig. 1A). The judgment of the high reliability of this docking model of the interaction of Zyesami (Fig. 1B) with SARS-CoV-2 nsp16 (Fig. 1C) was based on the score of modeling confidence. The overall global quality score of this predicted docking of Zyesami-nsp16 was 0.91633. This score indicated that this prediction is a more confident model. The docking structure of nsp10 in a complex with nsp16 was solved by molecular replacement at 1.8 Å (PDB code 6W4H) with Zyesami, as shown in Fig. (1D). Identifying key amino acid residues in the interaction between Zyesami and the SARS-CoV-2 nsp10/nsp16 complex. The docking model showed possible binding sites for Zyesami on nsp16 (Fig. 1). These potential

binding sites for Zyesami on SARS-CoV-2/COVID-19 nsp16 were visualized by PyMOL1.3. Based on this model of Zyesami and SARS-CoV-2/COVID-19 nsp16, several locations were identified as possible binding sites for this interaction (Figure 2). In addition, TYR⁶⁸²⁸ and GLY⁶⁸²⁹ residues were identified as possible binding sites on nsp16 for HIS¹ residue in Zyesami. In addition, there is contact between ASP³ of Zyesami and ASP⁶⁸²⁴, CYS⁶⁸²³, and LYS⁶⁸²² of nsp16. HIS⁶⁹⁷², GLU⁶⁹⁷¹, VAL⁶⁹³⁷, and CYS⁶⁸²³ in nsp16 were possible binding sites for Zyesami. The result also showed amino acid residues on Zyesami; VAL⁵, PHE⁶, TYR⁷, ASP⁸, ASN⁹, TYR¹⁰, TYR¹¹, and ARG¹² were predicted binding sites for nsp16 (Fig. 2A and Fig. 3).

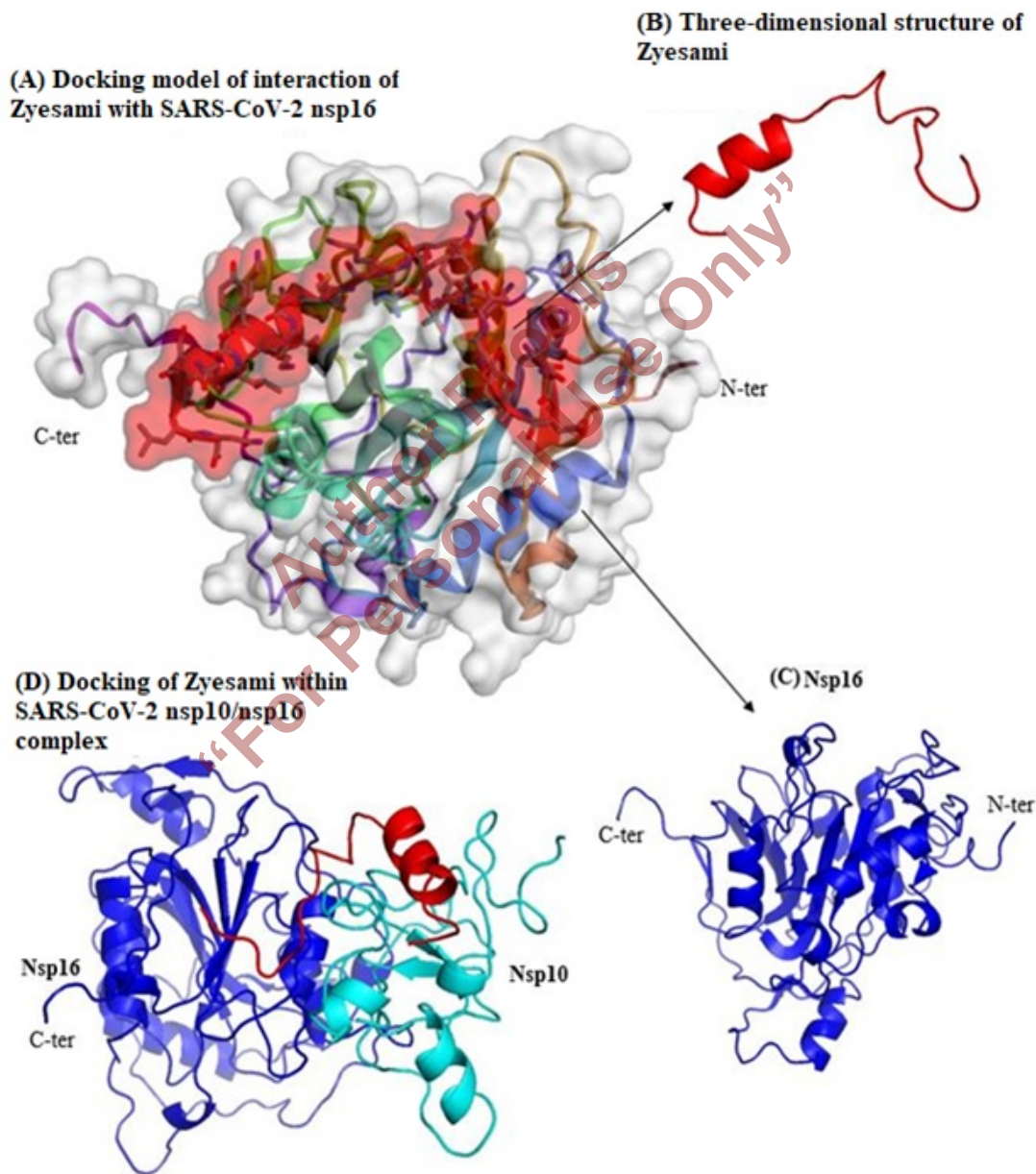


Fig. (1). Overall, the three-dimensional interaction structure of Zyesami with the SARS-CoV-2 nsp10/nsp16 complex is shown. (A) Docking model of Zyesami interaction with SARS-CoV-2 nsp16, 0.91633 (B) The three-dimensional structure of Zyesami, coloured in red. (C) Blue-colored three-dimensional structure of nsp16. (D) Docking of Zyesami within the SARS-CoV-2 nsp10/nsp16 complex, with nsp10 coloured in cyan and nsp16 coloured in blue. CABS-dock was used to produce this model of Zyesami-NSP16 interaction, and ProQdock validated it. The score is 0.91633, indicating that this docking model is high quality.

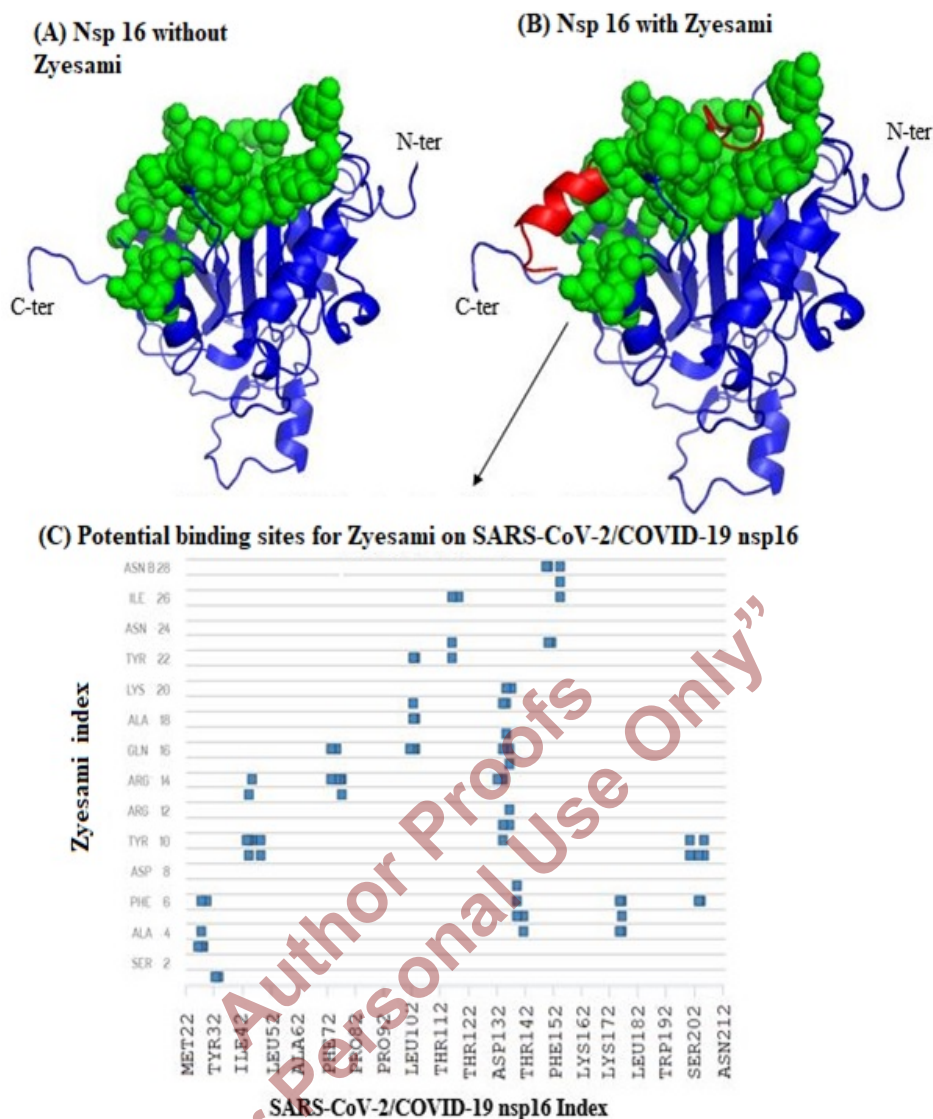


Fig. (2). shows potential Zyesami binding sites on SARS-CoV-2/ nsp16 residues. Residues of Zyesami on the Y axis and nsp16 residues on the X axis. (C) Residues required for the interaction of Zyesami and nsp16. Possible binding sites for this interaction appeared in blue squares.

4. DISCUSSION

The study of the interaction between SARS-CoV nsp10 and nsp16 was already established by many researchers [20, 22]. Yeast and mammalian two-hybrid systems were used to map this interaction [21, 22]. The three-dimensional structure of SARS-CoV 2, nsp10/nsp16 (PDB ID 6W4H), shows that essential interactions exist between nsp10 and nsp16 (Fig. 1D). Significant contact areas exist across nsp10 amino acid residues; Asn⁴⁰-Thr⁴⁷, Val⁵⁷-Pro⁵⁹, Gly⁶⁹-Ser⁷², Cys⁷⁷-Pro⁸⁴, Lys⁹³-Tyr⁹⁶ (Figure 1D). These results agreed with previous reports about the interaction domain of the SARS coronavirus [20, 22]. Also, Ke et al. (2012) showed that the area between Gln⁶⁵ and Pro¹⁰⁷ is vital for its interaction with nsp16, while the region between Val⁴² and Cys¹²⁰ of nsp10 is a vital area for the complete enzymatic activity of nsp16 [23]. The interaction study of Zyesami with the nsp16/nsp10 protein complex, shown as polar contacts between Chain A (in blue) and Chain C (in Red) are Asn²⁹⁹-

Ser⁴⁴⁰, Val²⁹⁷-Asn⁴⁴³, Gly¹⁴⁹-Tyr⁴³⁷, Gln¹⁵⁹-Lys⁴³⁰, Asn¹⁷⁸-Arg⁴²⁹, Ser¹⁴⁶-Arg⁴²⁹, Ser¹⁴⁶-Arg⁴²⁹, Lys¹⁴⁷-Arg⁴²⁹, Asr²²¹-Thr⁴²², Lys¹⁸³-Asp⁴²³, Lys¹⁸³-Asp⁴²³, and Gln²¹⁹-Asp⁴²³ the residues are shown of Chain A and Chain C respectively. PDBsum analysis is shown in (Fig. 4A), with a circular area representing the surface area of the protein, where Chain A (in Violet), Chain B (in Red), and Chain C (in dark yellow) are shown with reducing surface areas, respectively. The interaction between Chain A and Chain C is interesting (Fig. 4B). The extended interface regions in the circles indicate the respective chains interacting, and the shaded part signifies the interface area of the interacting chain. A total of 28 residues from Chain A and 18 from Chain C interact in various ways, with the red line representing a salt bridge, the blue line representing hydrogen bonds, and the orange line representing non-bonded interactions. DIMPLOT was used to visualize protein-protein interactions, representing the two-dimensional interaction of Zyesami and Chain A of the SARS-CoV-2 nsp16 protein, as shown in Fig. (4C).

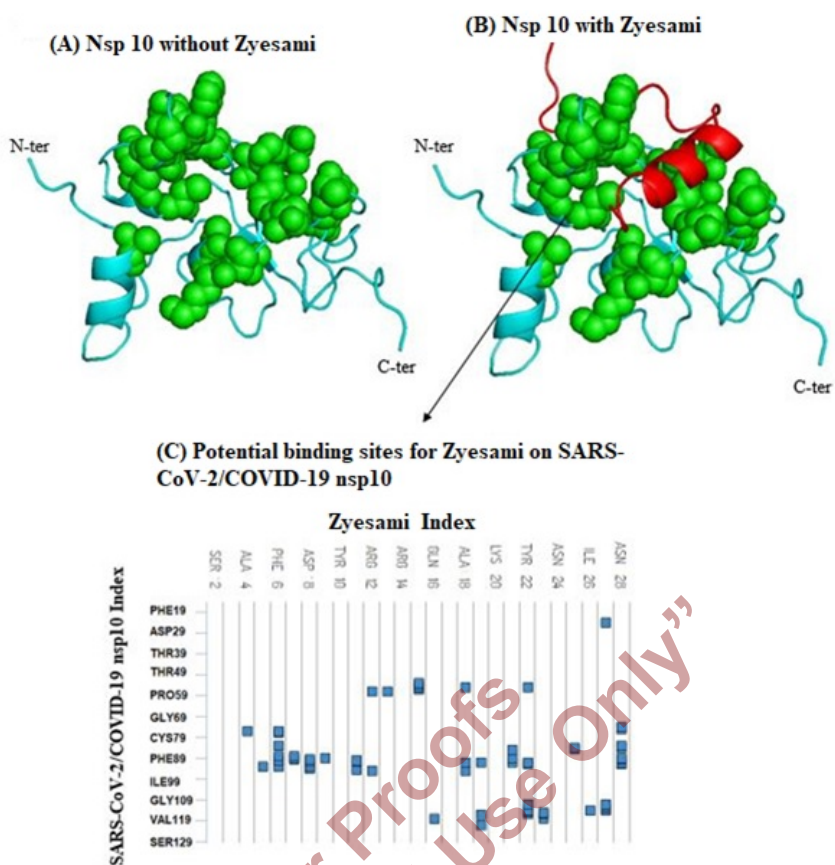


Fig. (3) Potential binding sites for Zyesami on SARS-CoV-2/COVID-19 nsp10. Residues of Zyesami on the X axis and nsp10 residues on the Y axis. (C) Residues required for the interaction of Zyesami and nsp10. Possible binding sites for this interaction appeared in blue squares.

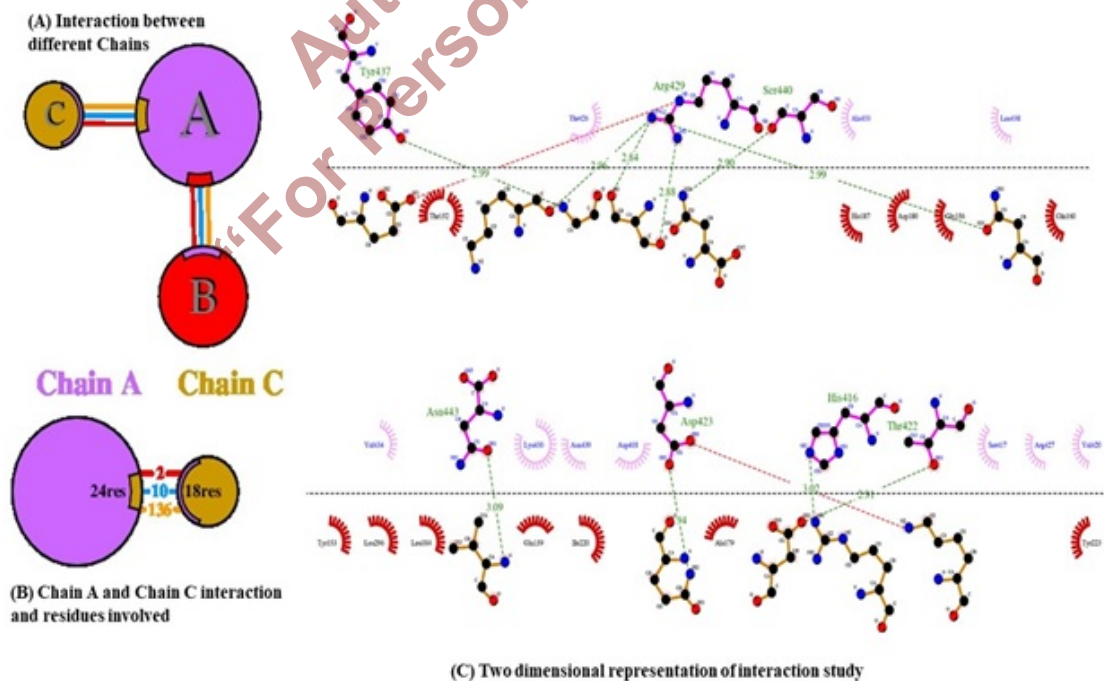


Fig. (4). Interaction study between the chains (A): Chain A (nsp16 in violet), Chain B (nsp10 in red) and Chain C (Zyesami in dark yellow). The circle area indicates the surface area of the protein chains, and non-bonded interactions, hydrogen bonds, and salt bridges are indicated as orange, light blue, and red lines, respectively. (B) In Chain A and Chain B, 24 and 18 residues interact with different bonds, respectively. (C) 2D representation of Chain A and Chain C's interaction, indicating residues of particular chains, bonds (H-Bonds in light blue and Salt Bridge in red) and bond lengths. A black dotted line indicates an interphase between chains.

Table 1. Residues involved in hydrogen bond interactions between Chain A and Chain C.

Chain A Residues	Atom Type	Distance (Å)	Chain C Residues	Atom Type
SER ¹⁴⁶	O	2.88 Å	ARG ⁴²⁹	NH2
SER ¹⁴⁶	OG	2.84 Å	ARG ⁴²⁹	NH1
LYS ¹⁴⁷	O	2.96 Å	ARG ⁴²⁹	NH1
GLY ¹⁴⁹	N	2.99 Å	TYR ⁴³⁷	OH
ASN ¹⁷⁸	OD1	2.99 Å	ARG ⁴²⁹	NH1
LYS ¹⁸³	NZ	2.78 Å	ASP ⁴²³	OD1
LYS ¹⁸³	NZ	2.82 Å	ASP ⁴²³	OD2
GLN ²¹⁹	NE2	2.94 Å	ASP ⁴²³	OD2
VAL ²⁹⁷	N	3.09 Å	ASN ⁴⁴³	OD1
ASN ²⁹⁹	ND2	2.90 Å	SER ⁴⁴⁰	O

There are ten hydrogen bonds between Chain A and Chain C as predicted from PDBSum, which include residues: Gly¹⁴⁹-Tyr⁴³⁷, Val²⁹⁷-Asn⁴⁴³, Lys¹⁴⁷-Arg⁴²⁹, Ser¹⁴⁶-Arg⁴²⁹, Asn¹⁷⁸-Arg⁴²⁹, Asn²⁹⁹-Ser⁴⁴⁰, Lys¹⁸³-Asp⁴²³, and Gln²¹⁹-Asp⁴²³, which were included in Table 1.

CONCLUSION

The structural bioinformatics analyses and results have indicated the potential binding specificity of Zyesami and nsp16. The data suggest that Zyesami's initial binding to NSp10 and NSp16 may occur in this manner. Moreover, this binding could significantly inhibit the 2-O-MTase activity of the SARS-CoV nsp10/16 complex.

ETHICS APPROVAL AND CONSENT TO PARTICIPATE

Not applicable.

HUMAN AND ANIMAL RIGHTS

Not applicable.

CONSENT FOR PUBLICATION

Not applicable.

AVAILABILITY OF DATA AND MATERIALS

Not applicable.

FUNDING

None.

CONFLICT OF INTEREST

The authors declare no conflict of interest.

ACKNOWLEDGEMENTS

The authors would like to thank the Deanship of Scientific Research at Shaqra University for supporting this work.

REFERENCES

- [1] Zumla, A.; Chan, JFW; Azhar, EI; Hui, DSC; Yuen, K-Y. Coronaviruses - drug discovery and therapeutic options. *Nat. Rev. Drug Discov.*, **2016**, *15*(5), 327-347. <http://dx.doi.org/10.1038/nrd.2015.37> PMID: 26868298
- [2] Chan, JFW; Chan, K-H; Kao, RYT; To, KKW; Zheng, B-J; Li, CPY. Broad-spectrum antivirals for the emerging Middle East respiratory syndrome coronavirus. *J. Infect.*, **2013**, *67*(6), 606-616. <http://dx.doi.org/10.1016/j.jinf.2013.09.029> PMID: 24096239
- [3] Dyall, J.; Coleman, C.M.; Hart, B.J.; Venkataraman, T.; Holbrook, M.R.; Kindrachuk, J.; Johnson, R.F.; Olinger, G.G., Jr; Jahrling, P.B.; Laidlaw, M.; Johansen, L.M.; Lear-Rooney, C.M.; Glass, P.J.; Hensley, L.E.; Frieman, M.B. Repurposing of clinically developed drugs for treatment of Middle East respiratory syndrome coronavirus infection. *Antimicrob. Agents Chemother.*, **2014**, *58*(8), 4885-4893. <http://dx.doi.org/10.1128/AAC.03036-14> PMID: 24841273
- [4] Omrani, AS; Saad, MM; Baig, K; Bahloul, A; Abdul-Matin, M; Alaidarous, AY. Ribavirin and interferon alfa-2a for severe Middle East respiratory syndrome coronavirus infection: A retrospective cohort study. *Lancet Infect. Dis.*, **2014**, *14*(11), 1090-1095. [http://dx.doi.org/10.1016/S1473-3099\(14\)70920-X](http://dx.doi.org/10.1016/S1473-3099(14)70920-X) PMID: 25278221
- [5] Temerozo, J.R.; Sacramento, C.Q.; Fintelman-Rodrigues, N.; Pão, C.R.R.; de Freitas, C.S.; da Silva Gomes Dias, S. The neuropeptides VIP and PACAP inhibit SARS-CoV-2 replication in monocytes and lung epithelial cells, decrease production of proinflammatory cytokines, and VIP levels are associated with survival in severe Covid-19 patients. *bioRxiv*, **2020**, 2020.07.25.220806.
- [6] Moody, T.W.; Ito, T.; Osefo, N.; Jensen, R.T. VIP and PACAP: Recent insights into their functions/roles in physiology and disease from molecular and genetic studies. *Curr. Opin. Endocrinol. Diabetes Obes.*, **2011**, *18*(1), 61-67. <http://dx.doi.org/10.1097/MED.0b013e328342568a> PMID: 21157320
- [7] Said, S.I.; Mutt, V. Polypeptide with broad biological activity: Isolation from small intestine. *Science*, **1970**, *169*(3951), 1217-1218. <http://dx.doi.org/10.1126/science.169.3951.1217> PMID: 5450698

- [8] Miyata, A.; Arimura, A.; Dahl, R.R.; Minamino, N.; Uehara, A.; Jiang, L.; Culler, M.D.; Coy, D.H. Isolation of a novel 38 residue-hypothalamic polypeptide which stimulates adenylate cyclase in pituitary cells. *Biochem. Biophys. Res. Commun.*, **1989**, *164*(1), 567-574.
[http://dx.doi.org/10.1016/0006-291X\(89\)91757-9](http://dx.doi.org/10.1016/0006-291X(89)91757-9) PMID: 2803320
- [9] Harmar, A.J.; Fahrenkrug, J.; Gozes, I.; Laburthe, M.; May, V.; Pisegna, J.R.; Vaudry, D.; Vaudry, H.; Waschek, J.A.; Said, S.I. Pharmacology and functions of receptors for vasoactive intestinal peptide and pituitary adenylate cyclase-activating polypeptide: IUPHAR review 1. *Br. J. Pharmacol.*, **2012**, *166*(1), 4-17.
<http://dx.doi.org/10.1111/j.1476-5381.2012.01871.x> PMID: 22289055
- [10] Datta, P.K.; Liu, F.; Fischer, T.; Rappaport, J.; Qin, X. SARS-CoV-2 pandemic and research gaps: Understanding SARS-CoV-2 interaction with the ACE2 receptor and implications for therapy. *Theranostics*, **2020**, *10*(16), 7448-7464.
<http://dx.doi.org/10.7150/thno.48076> PMID: 32642005
- [11] Lan, J.; Ge, J.; Yu, J.; Shan, S.; Zhou, H.; Fan, S.; Zhang, Q.; Shi, X.; Wang, Q.; Zhang, L.; Wang, X. Structure of the SARS-CoV-2 spike receptor-binding domain bound to the ACE2 receptor. *Nature*, **2020**, *581*(7807), 215-220.
<http://dx.doi.org/10.1038/s41586-020-2180-5> PMID: 32225176
- [12] Alnomasy, S.F. Virus-receptor interactions of SARS-CoV-2 spike-receptor-binding domain and human neuropilin-1 b1 domain. *Saudi J. Biol. Sci.*, **2021**, *28*(7), 3926-3928.
<http://dx.doi.org/10.1016/j.sjbs.2021.03.074> PMID: 33850424
- [13] Chen, Y.; Cai, H.; Pan, J.; Xiang, N.; Tien, P.; Ahola, T.; Guo, D. Functional screen reveals SARS coronavirus nonstructural protein nsp14 as a novel cap N7 methyltransferase. *Proc. Natl. Acad. Sci. USA*, **2009**, *106*(9), 3484-3489.
<http://dx.doi.org/10.1073/pnas.0808790106> PMID: 19208801
- [14] Bouvet, M.; Debarnot, C.; Imbert, I.; Selisko, B.; Snijder, E.J.; Canard, B.; Decroly, E. *In vitro* reconstitution of SARS-coronavirus mRNA cap methylation. *PLoS Pathog.*, **2010**, *6*(4), e1000863.
<http://dx.doi.org/10.1371/journal.ppat.1000863> PMID: 20421945
- [15] von Grothuss, M.; Wyrwicz, L.S.; Rychlewski, L. mRNA cap-1 methyltransferase in the SARS genome. *Cell*, **2003**, *113*(6), 701-702.
[http://dx.doi.org/10.1016/S0092-8674\(03\)00424-0](http://dx.doi.org/10.1016/S0092-8674(03)00424-0) PMID: 12809601
- [16] Bollati, M.; Milani, M.; Mastrangelo, E.; Ricagno, S.; Tedeschi, G.; Nonnis, S.; Decroly, E.; Selisko, B.; de Lamballerie, X.; Coutard, B.; Canard, B.; Bolognesi, M. Recognition of RNA cap in the Wesselsbron virus NS5 methyltransferase domain: Implications for RNA-capping mechanisms in Flavivirus. *J. Mol. Biol.*, **2009**, *385*(1), 140-152.
<http://dx.doi.org/10.1016/j.jmb.2008.10.028> PMID: 18976670
- [17] Kurcinski, M.; Jamroz, M.; Blaszczyk, M.; Kolinski, A.; Kmiecik, S. CABS-dock web server for the flexible docking of peptides to proteins without prior knowledge of the binding site. *Nucleic Acids Res.*, **2015**, *43*(W1), W419-24.
<http://dx.doi.org/10.1093/nar/gkv456> PMID: 25943545
- [18] Basu, S.; Wallner, B. Finding correct protein-protein docking models using ProQDock. *Bioinformatics*, **2016**, *32*(12), i262-i270.
<http://dx.doi.org/10.1093/bioinformatics/btw257> PMID: 27307625
- [19] Chen, Y.; Guo, D. Molecular mechanisms of coronavirus RNA capping and methylation. *Virol. Sin.*, **2016**, *31*(1), 3-11.
<http://dx.doi.org/10.1007/s12250-016-3726-4> PMID: 26847650
- [20] Chen, Y.; Su, C.; Ke, M.; Jin, X.; Xu, L.; Zhang, Z. Biochemical and structural insights into the mechanisms of SARS coronavirus RNA ribose 2'-O-methylation by nsp16/nsp10 protein complex. *PLoS Pathog.*, **2011**, *7*(10), e1002294.
<http://dx.doi.org/10.1371/journal.ppat.1002294> PMID: 22022266
- [21] Imbert, I.; Snijder, E.J.; Dimitrova, M.; Guillemot, J.-C.; Lécine, P.; Canard, B. The SARS-Coronavirus PLnc domain of nsp3 as a replication/transcription scaffolding protein. *Virus Res.*, **2008**, *133*(2), 136-148.
<http://dx.doi.org/10.1016/j.virusres.2007.11.017> PMID: 18255185
- [22] Pan, J.; Peng, X.; Gao, Y.; Li, Z.; Lu, X.; Chen, Y. Genome-wide analysis of protein-protein interactions and involvement of viral proteins in SARS-CoV replication. *PLoS One.*, **2008**, *3*(10), e3299.
<http://dx.doi.org/10.1371/journal.pone.0003299> PMID: 18827877
- [23] Ke, M.; Chen, Y.; Wu, A.; Sun, Y.; Su, C.; Wu, H. Short peptides derived from the interaction domain of SARS coronavirus non-structural protein nsp10 can suppress the 2'-O-methyltransferase activity of nsp10/nsp16 complex. *Virus Res.*, **2012**, *167*(2), 322-328.
<http://dx.doi.org/10.1016/j.virusres.2012.05.017> PMID: 22659295
- [24] Krafcikova, P.; Silhan, J.; Nencka, R.; Boura, E. Structural analysis of the SARS-CoV-2 methyltransferase complex involved in RNA cap creation bound to sinefungin. *Nat. Commun.*, **2020**, *11*(1), 3717.
<http://dx.doi.org/10.1038/s41467-020-17495-9> PMID: 32709887
- [25] Laurini, E.; Marson, D.; Aulic, S.; Fermeglia, M.; Pricl, S. Computational alanine scanning and structural analysis of the SARS-CoV-2 spikeprotein/angiotensin-converting enzyme 2 complex. *ACS Nano*, **2020**, *14*(9), 11821-11830.
<http://dx.doi.org/10.1021/acsnano.0c04674> PMID: 32833435
- [26] Hoffmann, M.; Kleine-Weber, H.; Schroeder, S.; Krüger, N.; Herrler, T.; Erichsen, S.; Schiergens, T.S.; Herrler, G.; Wu, N.H.; Nitsche, A.; Müller, M.A.; Drosten, C.; Pöhlmann, S. SARS-CoV-2 cell entry depends on ACE2 and TMPRSS2 and is blocked by a clinically proven protease inhibitor. *Cell*, **2020**, *181*(2), 271-280.e8.
<http://dx.doi.org/10.1016/j.cell.2020.02.052> PMID: 32142651
- [27] Letko, M.; Marzi, A.; Munster, V. Functional assessment of cell entry and receptor usage for SARS-CoV-2 and other lineage B betacoronaviruses. *Nat. Microbiol.*, **2020**, *5*(4), 562-569.
<http://dx.doi.org/10.1038/s41564-020-0688-y> PMID: 32094589
- [28] Tian, X.; Li, C.; Huang, A.; Xia, S.; Lu, S.; Shi, Z.; Lu, L.; Jiang, S.; Yang, Z.; Wu, Y.; Ying, T. Potent binding of 2019 novel coronavirus spike protein by a SARS coronavirus-specific human monoclonal antibody. *Emerg. Microbes Infect.*, **2020**, *9*(1), 382-385.
<http://dx.doi.org/10.1080/22221751.2020.1729069> PMID: 32065055
- [29] Daly, J.L.; Simonetti, B.; Klein, K.; Chen, K.E.; Williamson, M.K.; Antón-Plágaro, C.; Shoemark, D.K.; Simón-Gracia, L.; Bauer, M.; Hollandi, R.; Greber, U.F.; Horvath, P.; Sessions, R.B.; Helenius, A.; Hiscox, J.A.; Teesalu, T.; Matthews, D.A.; Davidson, A.D.; Collins, B.M.; Cullen, P.J.; Yamauchi, Y. Neuropilin-1 is a host factor for SARS-CoV-2 infection. *Science*, **2020**, *370*(6518), 861-865.
<http://dx.doi.org/10.1126/science.abd3072> PMID: 33082294
- [30] Cantuti-Castelvetri, L.; Ojha, R.; Pedro, L.D.; Djannat, M.; Franz, J.; Kuivanen, S.; van der Meer, F.; Kallio, K.; Kaya, T.; Anastasina, M.; Smura, T.; Levanov, L.; Szivovicza, L.; Tobi, A.; Kallio-Kokko, H.; Österlund, P.; Joensuu, M.; Meunier, F.A.; Butcher, S.J.; Winkler, M.S.; Mollenhauer, B.; Helenius, A.; Gokce, O.; Teesalu, T.; Hepojoki, J.; Vapalahti, O.; Stadelmann, C.; Balistreri, G.; Simons, M. Neuropilin-1 facilitates SARS-CoV-2 cell entry and infectivity. *Science*, **2020**, *370*(6518), 856-860.
<http://dx.doi.org/10.1126/science.abd2985> PMID: 33082293
- [31] Choudhary, S.; Malik, Y.S.; Tomar, S. Identification of SARS-CoV-2 cell entry inhibitors by drug repurposing using *in silico* structure-based virtual screening approach. *Front. Immunol.*, **2020**, *11*, 1664.
<http://dx.doi.org/10.3389/fimmu.2020.01664> PMID: 32754161
- [32] Fatma, B.; Kumar, R.; Singh, V.A.; Nehul, S.; Sharma, R.; Kesari, P. Alphavirus capsid protease inhibitors as potential antiviral agents for Chikungunya infection. *Antiviral Res.*, **2020**, *179*, 104808.
<http://dx.doi.org/10.1016/j.antiviral.2020.104808> PMID: 32380148
- [33] Wan, Y.; Shang, J.; Graham, R.; Baric, R.S.; Li, F. Receptor recognition by novel coronavirus from Wuhan: An analysis based on decade-long structural studies of SARS. *J. Virol.*, **2020**, *94*(7), e00127-e20.
<http://dx.doi.org/10.1128/JVI.00127-20> PMID: 31996437
- [34] Clark, M.J.; Miduturu, C.; Schmidt, A.G.; Zhu, X.; Pitts, J.D.; Wang, J.; Potisopon, S.; Zhang, J.; Wojciechowski, A.; Hann Chu, J.J.; Gray, N.S.; Yang, P.L. GNF2 inhibits dengue virus by target-

- ing Abl kinases and the viral e protein. *Cell Chem. Biol.*, **2016**, 23(4), 443-452.
<http://dx.doi.org/10.1016/j.chembiol.2016.03.010> PMID: 27105280
- [35] Chakraborty, A.; Koldobskiy, M.A.; Bello, N.T.; Maxwell, M.; Potter, J.J.; Juluri, K.R.; Maag, D.; Kim, S.; Huang, A.S.; Dailey, M.J.; Saleh, M.; Snowman, A.M.; Moran, T.H.; Mezey, E.; Snyder, S.H. Inositol pyrophosphates inhibit Akt signaling, thereby regulat-
- ing insulin sensitivity and weight gain. *Cell*, **2010**, 143(6), 897-910.
<http://dx.doi.org/10.1016/j.cell.2010.11.032> PMID: 21145457
- [36] Cheng, H.; Lear-Rooney, C.M.; Johansen, L.; Varhegyi, E.; Chen, Z.W.; Olinger, G.G.; Rong, L. Inhibition of ebola and marburg virus entry by G protein coupled receptor antagonists. *J. Virol.*, **2015**, 89(19), 9932-9938.
<http://dx.doi.org/10.1128/JVI.01337-15> PMID: 26202243

DISCLAIMER: The above article has been published, as is, ahead-of-print, to provide early visibility but is not the final version. Major publication processes like copyediting, proofing, typesetting and further review are still to be done and may lead to changes in the final published version, if it is eventually published. All legal disclaimers that apply to the final published article also apply to this ahead-of-print version.

Author Proofs
"For Personal Use Only"